Calorimetry

in particle physics experiments

7. Signal Chain, Readout Electronics & Calibration

Course roadmap

- **Week 1 (Foundations)**
  - ✓ Lecture 1: Why calorimetry?
  - ✓ Lecture 2: EM shower physics
- **Week 2 (Physics depth)**
  - ✓ Lecture 3: Hadronic shower physics
  - ✓ Lecture 4: Energy resolution from first principles
- **Week 3 (Technology)**
  - ✓ Lecture 5: Calorimeter Technologies (real-life EM and Hadronic calorimeters)
  - ✓ Lecture 6: Calorimeter Design
- **Week 4 (Systems & Future)**
  - ✓ Lecture 7: Signal chain, readout, calibration
  - ✓ Lecture 8: Future calorimetry

Today's Lecture

- Week 4 (Systems & Future)
  - ✓ Lecture 7: Signal chain, readout, calibration
    - *Signal chain and electronics → from shower energy deposit to ADC counts.*
      - *7.1 Signal formation in calorimeters (ionization, scintillation)*
      - *7.2 Preamplifier & signal shaping (CSA topology; CR-RC shaping; noise bandwidth)*
      - *7.3 Dynamic range and ADC (multiple gain system, MeV to TeV coverage)*
      - *7.4 Optimal filtering (amplitude and time extraction; pile-up and HL-LHC challenges)*
      - *7.5 Trigger primitives*
    - *EM and HAD calibration → from ADC counts to calibrated energy to objects*
      - *7.6 Calibration chain*
      - *7.7 Test-beam calibration (absolute scale, module inter-calibration)*
      - *7.8 In-situ calibration (muon MIP; $\pi^0 \rightarrow \gamma\gamma$; $Z \rightarrow ee$; E/p method)*
      - *7.9 HAD calibration (cell weighting; software compensation; jet energy scale (JES))*
  - ✓ Lecture 8: Future calorimetry

7.1

Signal Formation in Calorimeters

From shower to measurable signal

- Reminder: LAr ionization physics
  - ✓ Q ~ E_{dep}/W_{ion} ~ few × 10^7 e^-/cell
  - ✓ d = 2 mm ; HV = 2 kV ; E = 1 kV/mm
  - ✓ v_d ~ 5 mm/μs → τd = d/vd = 400 ns
- Electronics challenge: ~400 ns drift time spans ~16 LHC bunch crossings at 40 MHz!
  - ✓ Problem 1: pile-up charge from successive BX accumulates on electrode → need to restore baseline between crossings
  - ✓ Problem 2: naive integration aliases previous-BX signals into current measurement → offline correction alone is insufficient
  - ✓ Solution: bipolar CR-RC shaping shapes the 400 ns triangular current into a ~50 ns peaked bipolar pulse; negative lobe cancels DC pile-up baseline; full signal reconstructed from ~5 samples by OFC
- Contrast with (modern, fast) crystal scintillation (e.g CMS ECAL PbWO4)
  - ✓ τ_1 ~ 10 ns (80%); τ_2 ~ 30 ns
  - ✓ ~80% collected in one 25 ns BX → much simpler shaping requirement
  - ✓ In this case, shaping addresses a noise problem → *integration* toward *longer* pulses!

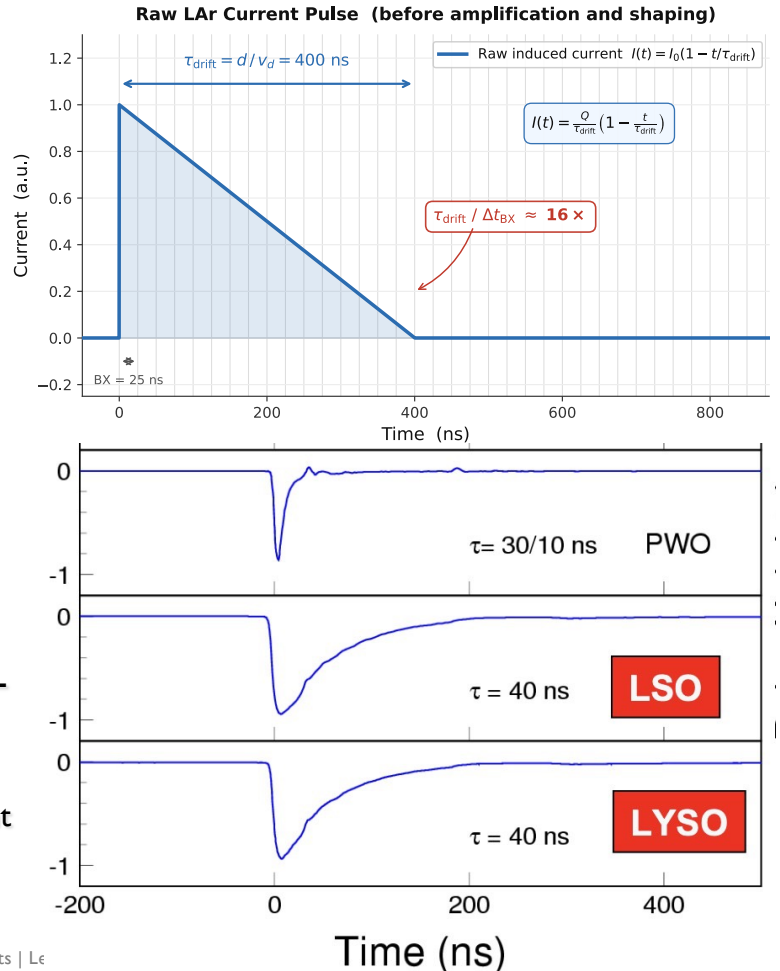

Pile-up

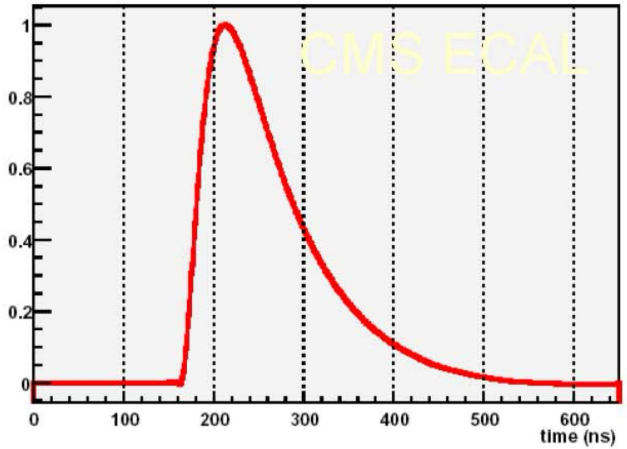
CMS ECAL
1
0.8
0.6
0.4
0.2
0
0
100
200
300
400
500
600
time (ns)

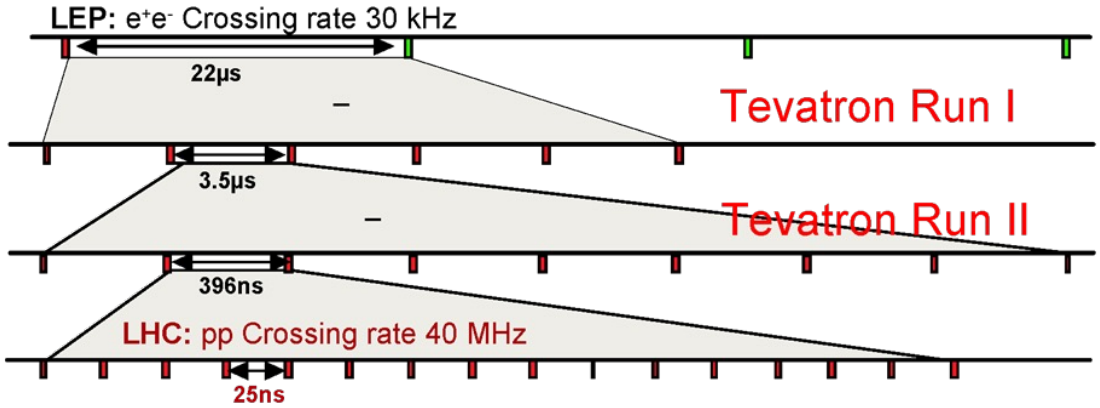
LEP: e+e- Crossing rate 30 kHz
22μs
Tevatron Run I
3.5μs
Tevatron Run II
396ns
LHC: pp Crossing rate 40 MHz
25ns

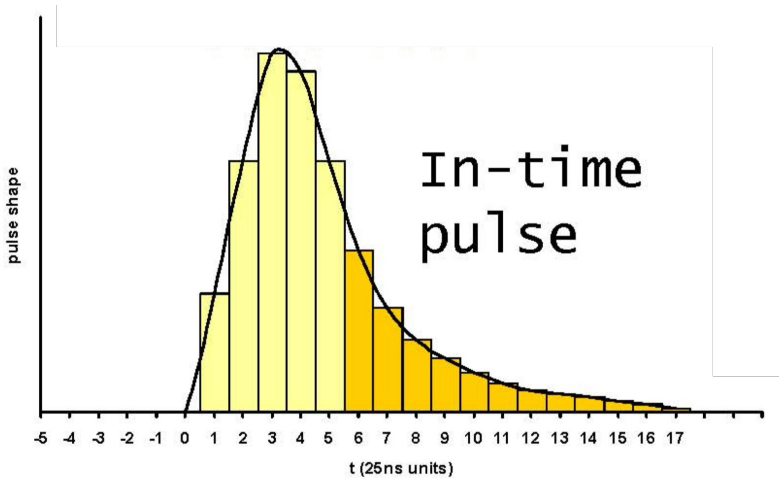
In-time pulse
pulse shape
-5 -4 -3 -2 -1 0 1 2 3 4 5 6 7 8 9 10 11 12 13 14 15 16 17
t (25ns units)

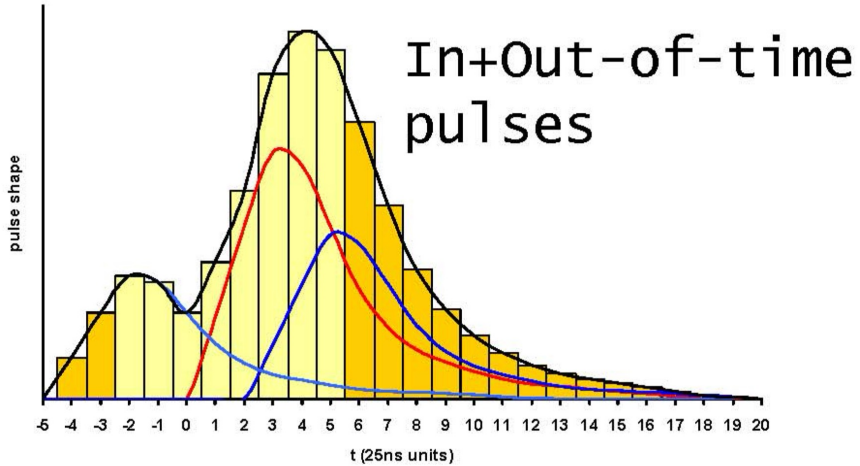
In+Out-of-time pulses
pulse shape
-5 -4 -3 -2 -1 0 1 2 3 4 5 6 7 8 9 10 11 12 13 14 15 16 17 18 19 20
t (25ns units)

Full signal chain

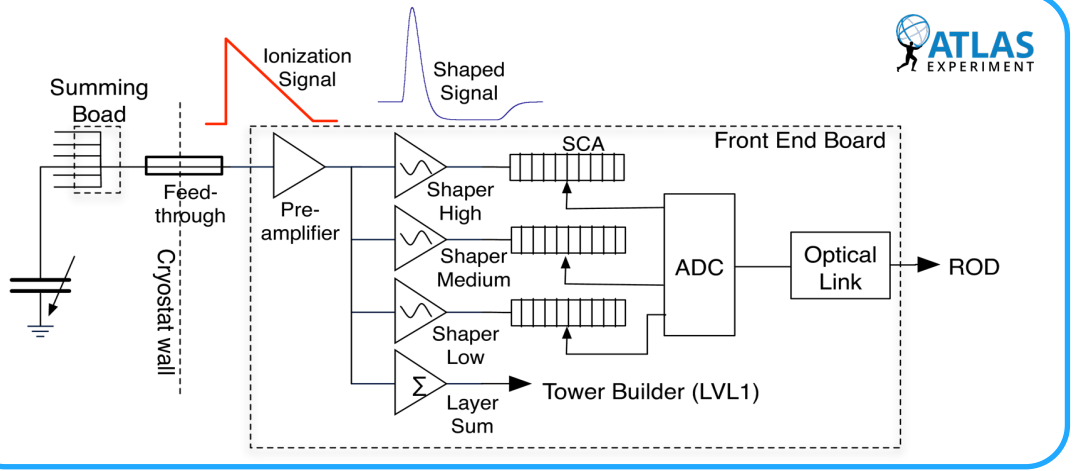

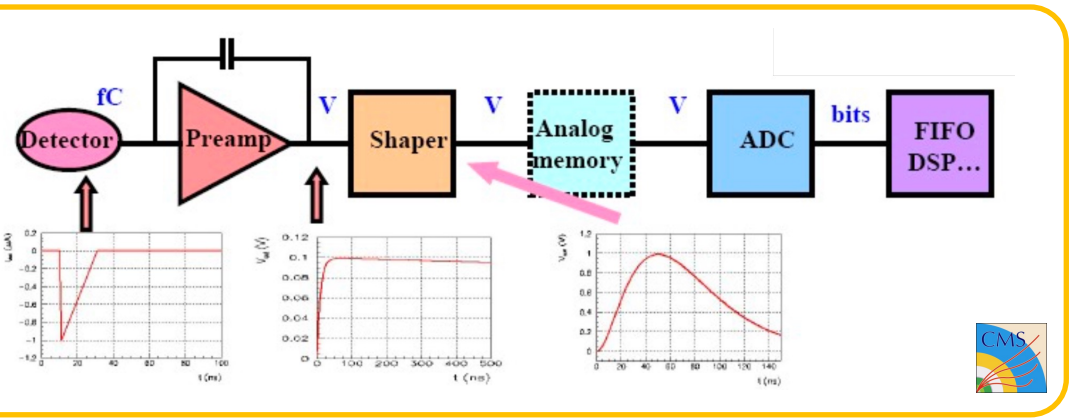

shower

↓

ionization/scintillation
(in a given cell)

↓

preamplifier

↓

Signal shaping
(e.g. CR-RC^n)

↓

ADC
(e.g. 40 MHz @ LHC)

↓

amplitude reconstruction
(e.g. Optimal Filtering)

↓

"calibrated" energy
from amplitude

7.2

Preamplifier, Noise Sources & Signal Shaping

Preamplifier: from detector signal to shaped voltage

- **What a preamplifier must do**
  - ✓ Convert the detector signal (charge Q or current I) to a measurable voltage with minimum added noise
    - LAr: integrates the triangular current pulse
      - total charge Q = ∫I dt
    - Crystal (APD/SiPM): current proportional to scintillation light yield
  - ✓ Key requirements: low input-referred noise, fast response, large dynamic range (MeV → TeV)

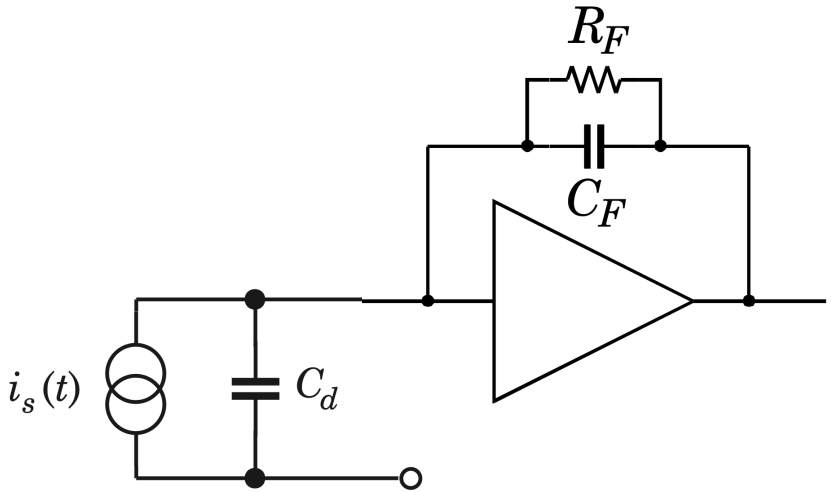

- **Charge-Sensitive Amplifier (CSA) topology**
  - ✓ Integrating amplifier with feedback capacitor C_f: output voltage $V_{out} = Q / C_f$ independent of detector capacitance C_{det}
  - ✓ Noise (ENC) ∝ C_{det} → minimise detector capacitance
    - E.g. in LAr calorimeters cell size and electrode geometry are noise-driven design choices
  - ✓ Feedback resistor R_f: sets slow discharge $\tau = R_f C_f$ (baseline recovery); also source of parallel (current) noise
  - ✓ Preamplifier output: exponential step (CSA) → effectively and integration step, followed by CR-RC^n shaper

Pulse shaping

- **Why shaping? Two conflicting goals**
  - ✓ Filter noise to increase S/N ratio → integrate for longer time (e.g. CMS ECAL)
  - ✓ Avoid pulse overlap (and reduce pile-up effect) → speedup pulse (e.g. ATLAS LAr)
    - In some case, zero-integral bipolar pulse to guarantee baseline (e.g. ATLAS LAr)
- **How? CR-RC^n shaping network**
  - ✓ CR (high-pass) = "differentiator"
    - Removes DC component and pile-up baseline; sets pulse duration
  - ✓ RC (low-pass) = "integrator"
    - Limits bandwidth → reduces noise → smooths pulse (increase rise time)

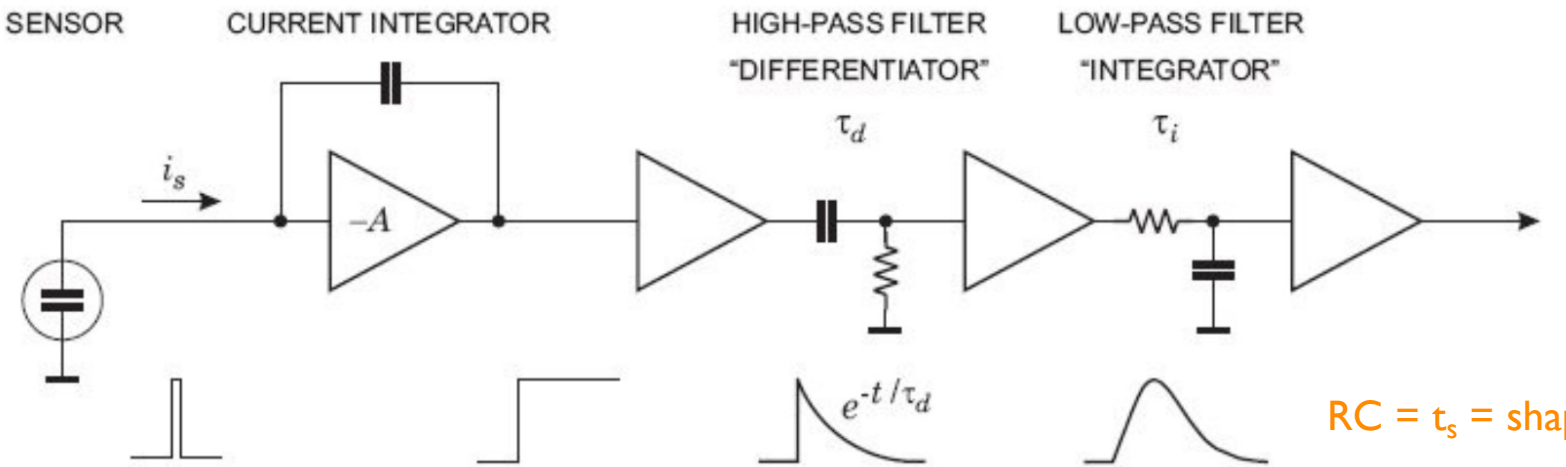

RC = t_s = shaping time

Electronic noise sources and shaping time optimization

- **Three noise sources in calo readout**
  - ✓ Series noise
    - Voltage noise of preamplifier input transistor ~ C_{det}^2/t_s
  - ✓ Parallel noise
    - Current noise (leakage, feedback resistor) ~ t_s
  - ✓ 1/f noise
    - FET channel fluctuations; independent of t_s

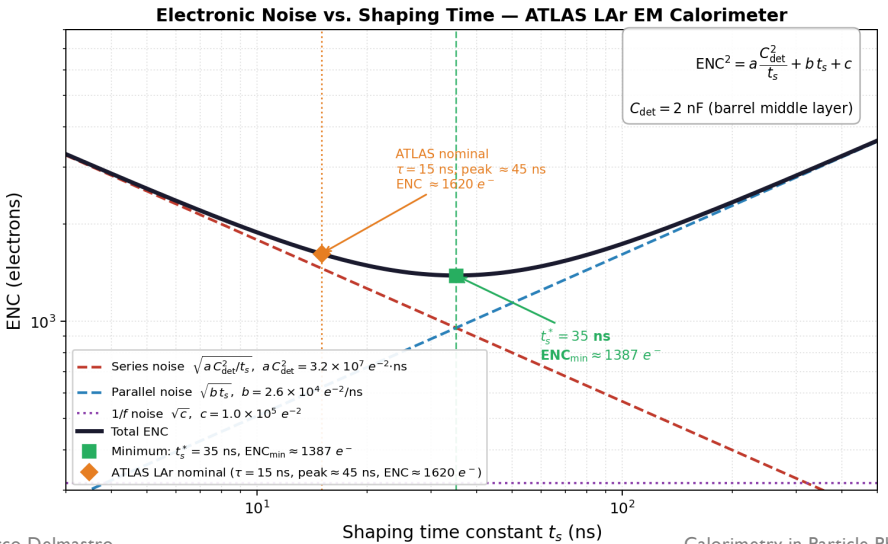

- **Equivalent Noise Charge (ENC)**
  - ✓ Combined noise in units of electrons or coulombs

$$\mathrm{ENC}^2 = a\frac{C_{\mathrm{det}}^2}{t_s} + bt_s + c$$

  - ✓ Optimal shaping time minimizes total ENC

$$t_s^* = \sqrt{\frac{a}{b}}C_{\mathrm{det}}$$

  - ✓ Example: ATLAS LAr
    - C_{det} ~ 1-5 nF (accordion electrode capacitance)
    - ENC ~ 20-60 MeV per cell at optimal shaping time (50 ns for ATLAS)
    - t_s^* ~ 35 ns
      - …but ATLAS LAr operates at t_s ~ 15 ns (why?)

Example of shaped signals

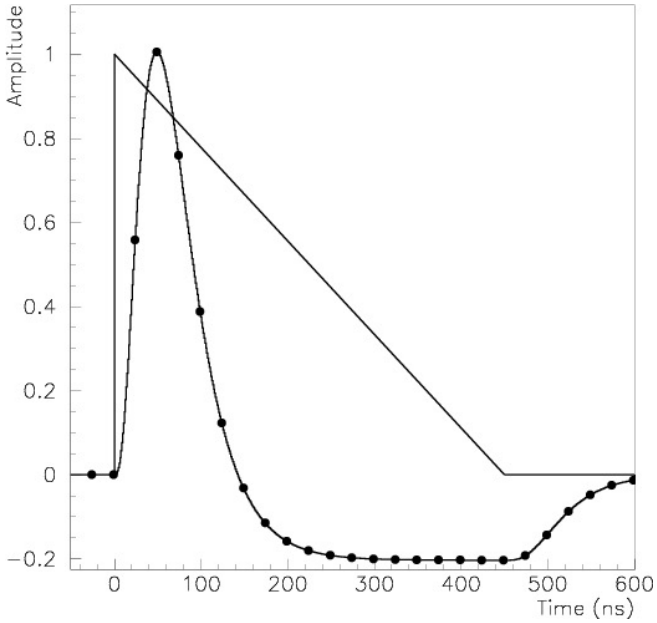

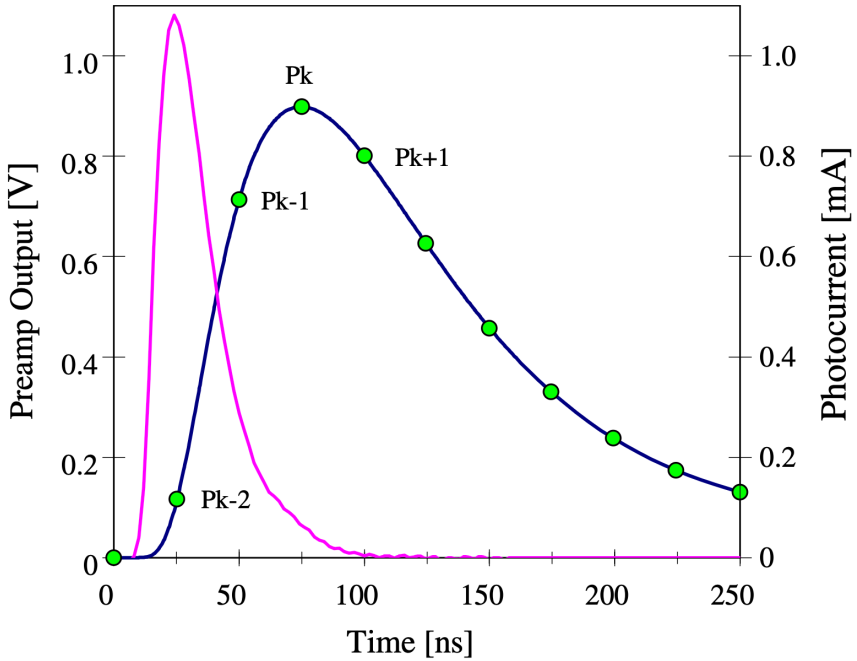

- ATLAS LAr
  - ✓ C_{det} ~ 1-5 nF (accordion electrode capacitance)
  - ✓ Long pulse: very sensitive to PU
  - ✓ Bipolar shaping with CR-RC^2 network
    - Why bipolar? More on this later..

- CMS ECAL
  - ✓ C_{det} ~ 200 pF (capacitance of interconnections and APDs)
  - ✓ Short pulse, low photo-electron yield: very sensitive to noise
  - ✓ Monopolar shaping with CR-RC network

Electronic noise vs Pileup noise

Shaping time compromise between electronic noise, bunch crossing and PU noise!

PU noise depends on instantaneous luminosity: had to "guess" best operating point…

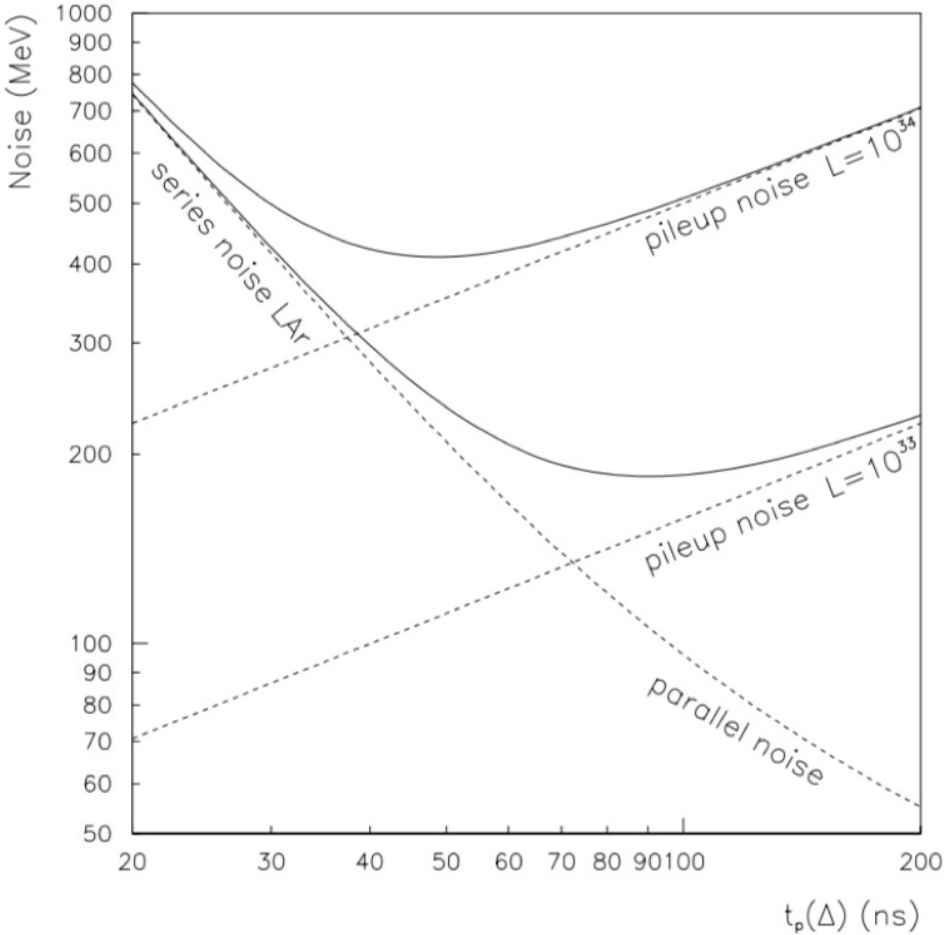

Digitized pulse + digital filtering amplitude reconstruction ("Optimal Filtering") can address varying luminosity conditions

7.3

Dynamic Range and ADC

Physics dynamic range and impact on ADC

- LHC EM calorimeter dynamic range: from noise (few MeV) to highest-energy deposits (few TeV)
  - ✓ Minimum signal: tau lepton decay products ~ 1-2 GeV; noise ~ 50 MeV
  - ✓ Maximum signal: 3.5 TeV electron or very energetic jets (rare but must not saturate)
  - ✓ Dynamic range needed: ~16 bits = 65536 steps → standard 12-bit ADC insufficient

- Solution: multiple gain system
  - ✓ e.g. ATLAS LAr 3-gain system
    - High gain (HG): x64 amplification for low-energy signals (E<~12 GeV)
    - Medium gain (MG): x8 amplification for intermediate energies
    - Low gain (LG): x1 for high-energy signals (E >~100 GeV)
    - Gain switching: all three gains always digitized; reconstruction uses highest unsaturated gain
  - ✓ 12-bit ADC at 40 MHz: 4096 steps per gain; with 3 gains: effective 18-bit dynamic range

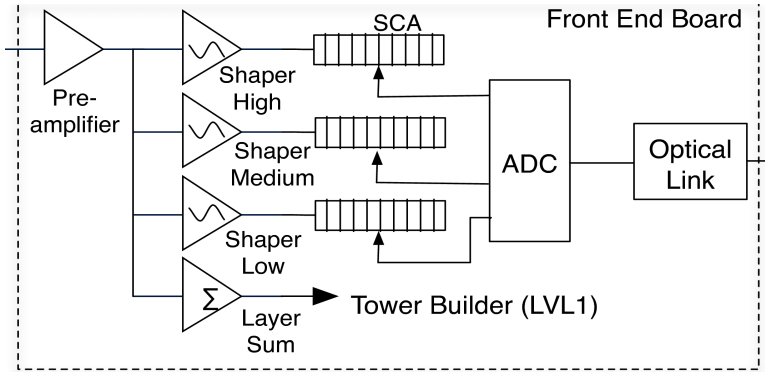

- Drawback: gain intercalibration!
  - ✓ In ATLAS Run 1-3 Z→ee electrons shower cells mostly in High Gain, H →**γγ** photon shower cells mostly in Medium Gain! Significant impact on photon calibration (and Higgs mass)…
  - ✓ Phase 2 electronic upgrade for HL-LHC: only 2 gains!

7.4

Optimal Filtering

Optimal Filtering amplitude reconstruction

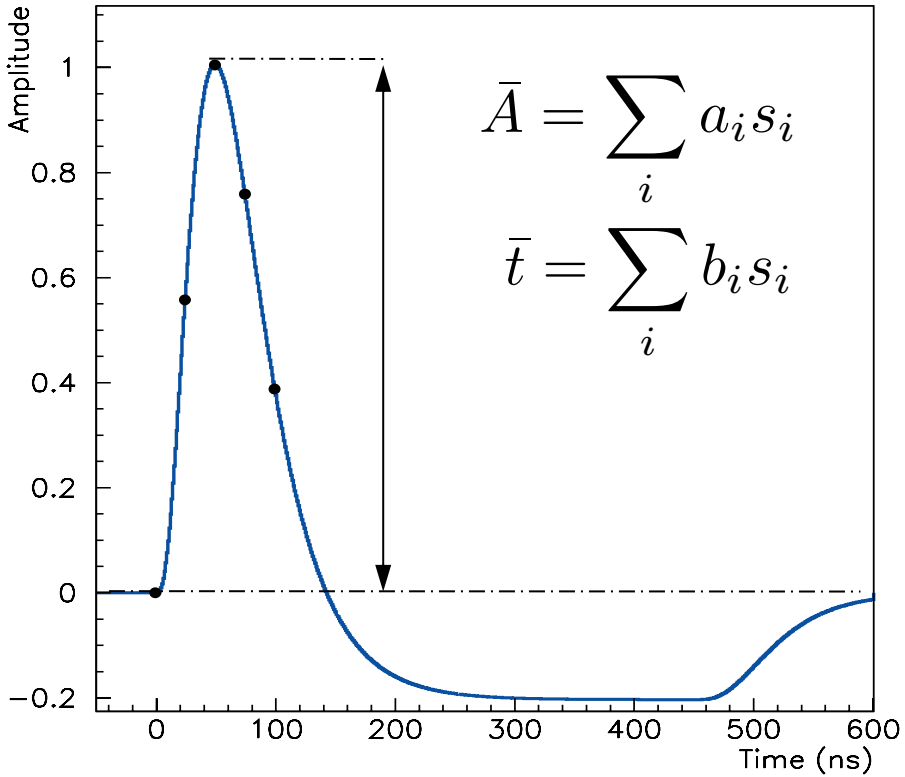

- Problem: extract amplitude A and time t from a few (noisy) digitized samples
  - ✓ Samples (g = shaped pulse shape)

$$s_i = Ag(t_i - t_0) + n_i$$

  - ✓ Maximum likelihood estimator for A: minimize

$$\chi^2 = \sum_i (s_i - Ag_i)^2 / \sigma_i^2$$

- Optimal Filter Coefficients (OFC): precomputed weights a_i for amplitude and b_i for time
  - ✓ OFC derivation: minimize noise contribution to A given the pulse shape g_i and noise correlations

$$\langle n_i \rangle = 0 \quad \langle n_i n_j \rangle = R_{ij}$$

- OFC derivation requires: (1) pulse shape g(t); (2) noise autocorrelation matrix R_{ij}

Optimal Filtering as digital shaping

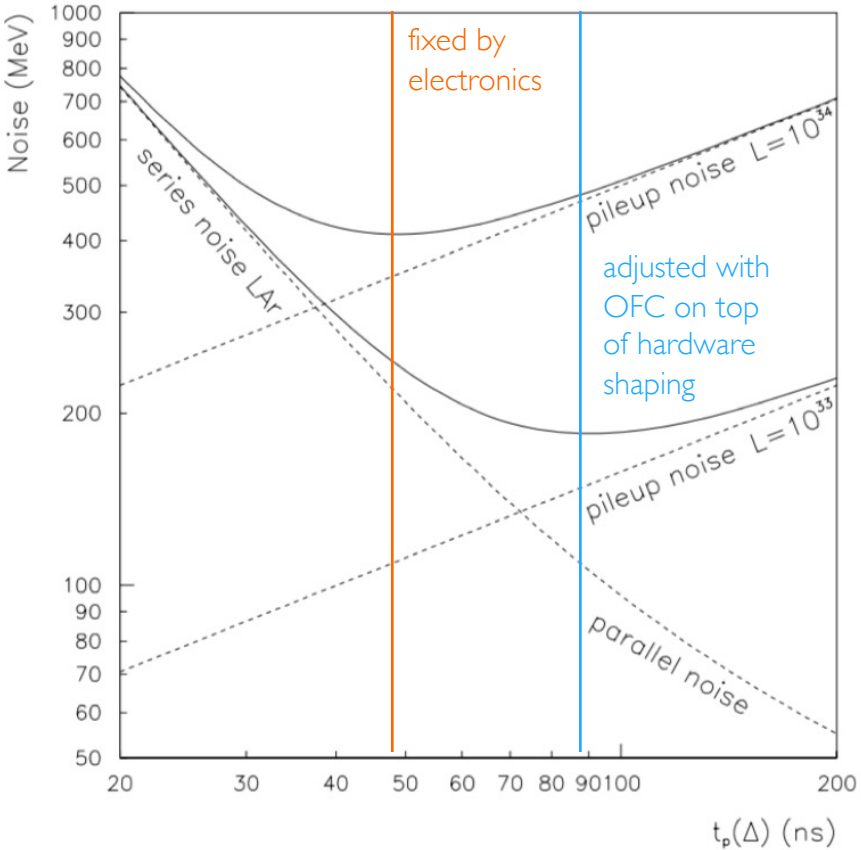

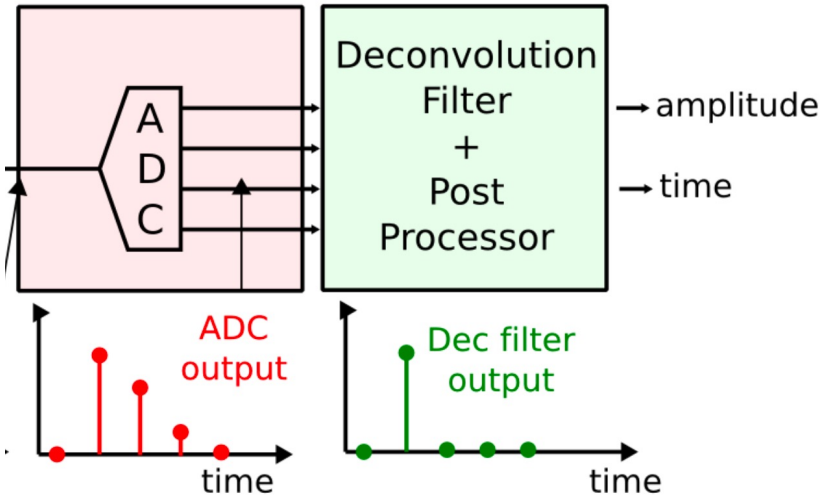

$$\bar{A} = \sum_i a_i s_i$$

More details on OFC optimization here:

Nuclear Instruments and Methods in Physics Research A 338 (1994) 467–497
North-Holland

NUCLEAR INSTRUMENTS & METHODS IN PHYSICS RESEARCH
Section A

Signal processing considerations for liquid ionization calorimeters in a high rate environment **

W.E. Cleland *, E.G. Stern [1]

Department of Physics and Astronomy, University of Pittsburgh, Pittsburgh, PA 15260, USA

(Received 13 July 1993)

We present the results of a study of the effects of thermal and pileup noise in liquid ionization calorimeters operating in a high luminosity environment. The method of optimal filtering of multiply-sampled signals to obtain timing and amplitude from calorimeter signals is described. This method has some advantages over the traditional method of sampling the peak of a shaped signal, which include a reduced sensitivity to channel-to-channel variations in the pre-filter shaping parameters and good performance over a wide range of operating conditions. Analytic expressions for the variance of amplitude and timing measurements are found through a frequency domain approach. Implications for the choice of pre-filter shaping time, number and position of the samples, and digitization accuracy are discussed.

Pileup in system with bipolar shaping

3.2.2. Pileup in systems with bipolar shaping

In the situation where pileup noise is continuously distributed in time, Campbell's theorem [8–9] may be used to find the pileup variance. However, at a collider, where the signals are generated at fixed intervals, it is necessary to use a discrete sum in calculating the effect of pileup noise. The expression for this case is derived in the appendix.

From Eq. (99) we see that the expression for the pileup variance is

$$\sigma_p^2 = \rho_p^2 T_c \sum_{i=-\infty}^{\infty} g^2(t_i) = \rho_p^2 S_p \qquad (17)$$

in which $\rho_p^2 = \mathrm{Var}(E)/T_c$ is the variance of the energy deposition in the calorimeter per crossing, T_c is the time between crossings, $g(t)$ is the signal waveform and S_p, called the "pileup sum" in this paper, is the discrete form of the so-called "pileup integral",

$$I_{2p} = \int_{-\infty}^{\infty} g^2(t)\, dt. \qquad (18)$$

The quantity ρ_p, called the pileup noise density, is that part of σ_p which is independent of the signal processing parameters. The dimensions of ρ_p are $E/\sqrt{T}$ while S_p has dimensions of T, reflecting the time interval

- Bipolar shaping ideally ensures pileup noise has zero average

$$\langle n_i \rangle = 0$$

- Pileup noise autocorrelation R_{ij} can be compute from bipolar pulse shape

$$R^{\mathrm{pileup}}(t) \propto \int g(u)g(t-u)du$$

- But… in real life application (e.g. LHC) pulse shape is not perfectly known (bias) and not continuously know (only samples, not infinite bunch trains…)

$$\int g(t)dt = 0 \qquad \sum g(t_i) \neq 0$$

In-time and out-of-time pileup effect

- **Ideally, infinite bunch trains with same luminosity per bunch**
  - ✓ Average pileup energy per cell = 0
  - ✓ Pileup fluctuations translate in noise per cell
    - dominant w.r.t. electronics noise for eta>2.5

- **In real life, bunch train structure and bunch-to-bunch luminosity variations**

$$\sum g(t_i) \neq 0$$

  - ✓ No cancellation of out-of-time pileup shifts for first bunches
  - ✓ Residual shifts for bunches with luminosity different from average
  - ✓ Only the first effect simulated in ATLAS MC
- ATLAS solutions: correction computed from pulse shape, OFC, bunch-per-bunch luminosity (data) or bunch structure (MC), and average energy per cell for in-time only energy deposit

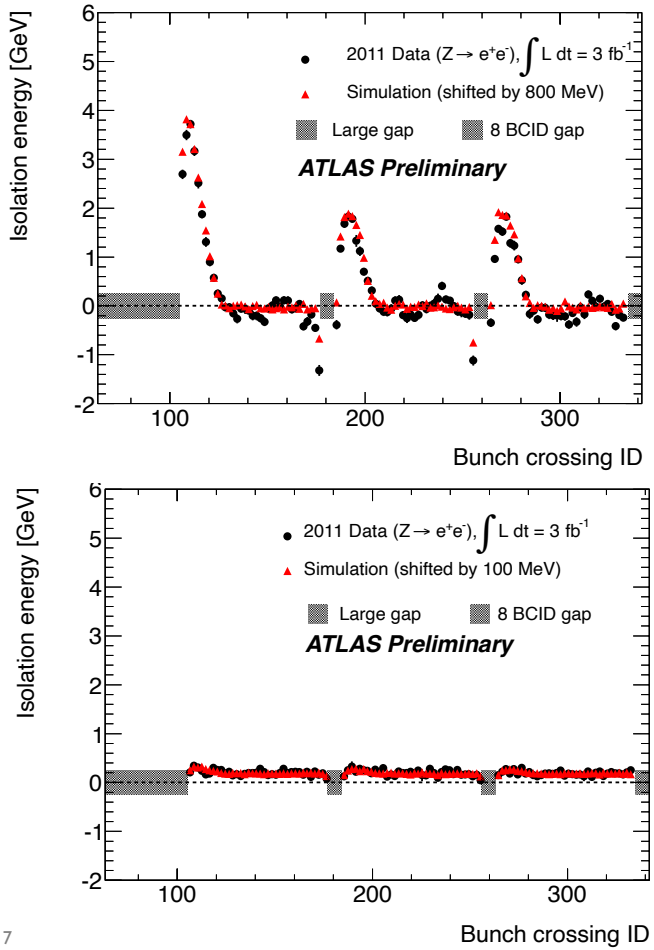

OFC at HL-LHC

- Standard OFC assumes single isolated pulse and only pile-up ”noise”
  - ✓ At HL-LHC (200 pile-up events): every cell will have significant (not noise-like) contributions from multiple BX: energy from previous BX introduce baseline shift
- PU-induced baseline shift mitigation strategies
  - ✓ Add OFC term for baseline shift
  - ✓ Machine learning based estimator (being tested for Phase-2)
    - e.g. ATLAS Phase 2 studying Recurrent Neural Network reconstruction

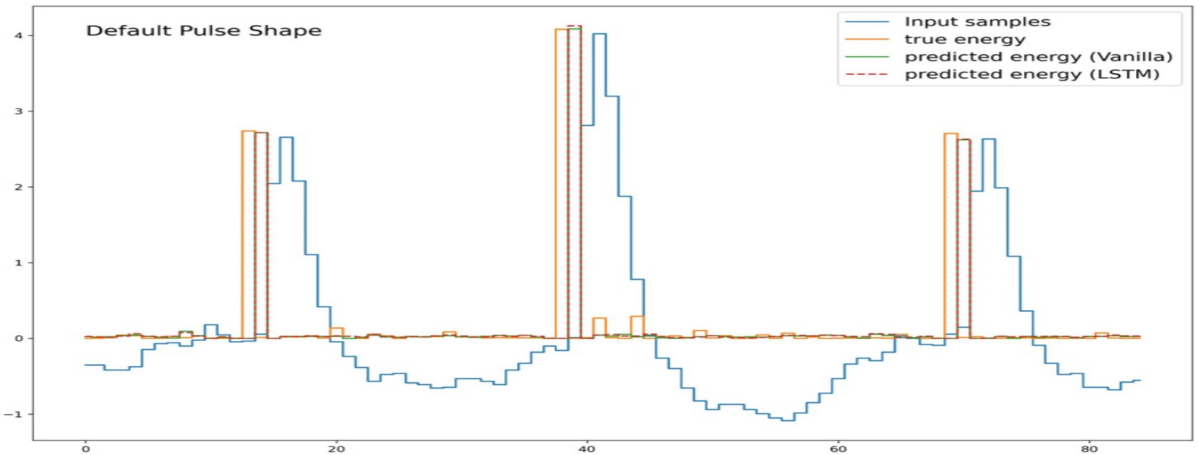

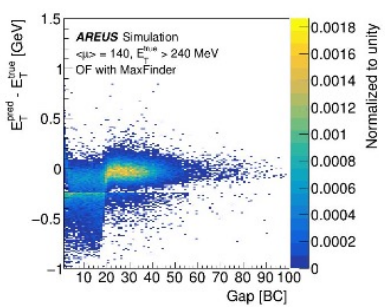

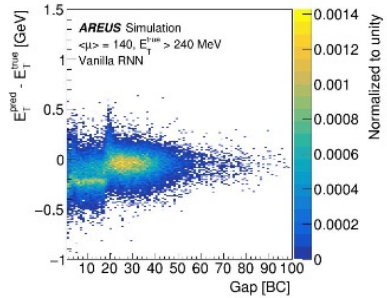

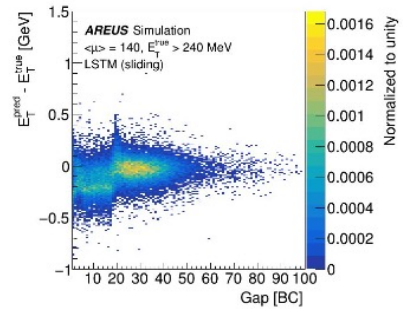

7.5

Trigger Primitives

From readout to trigger: Level 1 trigger primitives

- Trigger needed at hadron colliders because of overwhelming QCD background
- Trigger systems usually build on cascading levels: Level-1 at hardware level to be fast
  - ✓ Example: ATLAS L1 trigger decision in 2.5 us
- Calorimetes are fundamental component of Level-1 triggers
  - ✓ Works on reduced granularity sums and approximate reconstruction to speed up decision
  - ✓ Reduced granularity depends on electronics processing capabilities!
  - ✓ Example:
    - ATLAS LAr Phase 0 (Run 1-2): Tower Builder Boards summed analogue signals before digitization
    - ATLAS LAr Phase 1 (Run 3): LATOME digital processors allows for Super Cells with 10x finer trigger granularity

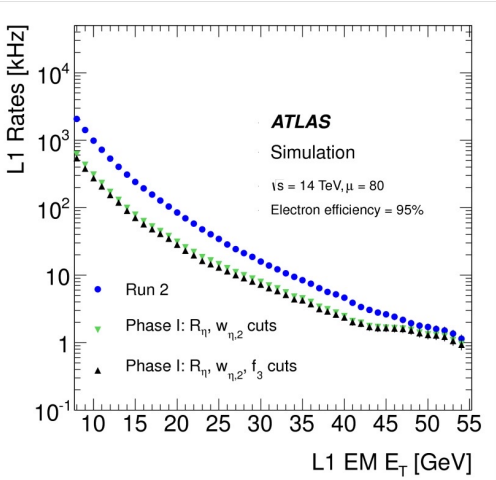

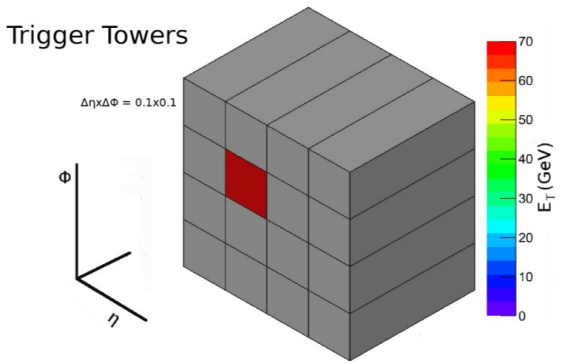

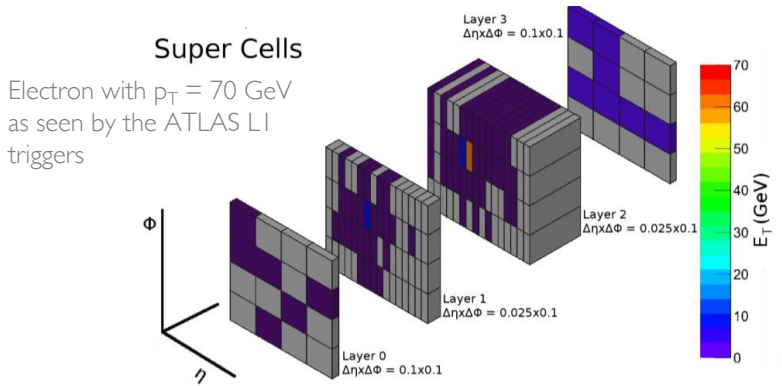

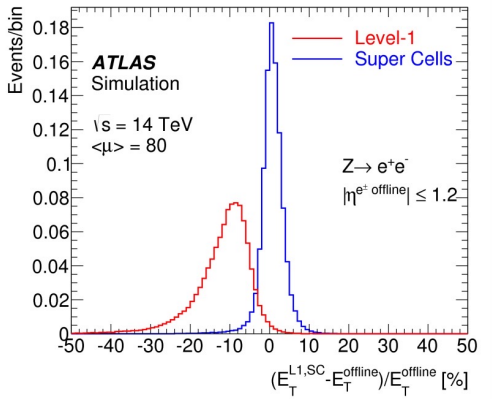

7.6

Calibration Chain

Cell energy calibration

- From pulse amplitude (e.g. from OF reconstruction) to calibrated energy in a cell

$$E_j^{\text{cell}} = F_{\mu A \to \text{MeV}} \cdot \frac{1}{f_{\text{samp}}} \cdot c_j \cdot G_j \cdot A_j$$

$F_{\mu A \to \text{MeV}}$: Overall physics response of detector (light/energy, current/energy). Can be simulated, but final values usually from test-beam

$\frac{1}{f_{\text{samp}}}$: Sampling fraction correction (from simulation)

Only for sampling calorimeters; usually considered constant at this stage, but can have energy dependence if material in front of calo: addressed at next stage

G_j: Electronic response [uA/ADC]; needs to be monitored vs time (e.g. pulse injection)

c_j: Cell response uniformity (e.g. crystal transparency); if drifting in time (e.g. radiation damage) needs to be monitored vs time, e.g. laser monitoring, radioactive sources for HAD calorimeters); (in ATLAS LAr corrects for bias from calibration signal injection point)

Cluster energy calibration

- Shower energy deposit covers more than one cell (by construction!)

In-situ global energy scale using "standard candle" processes (e.g Z→ee)

Clustering (size can static or dynamic, per layer is present and optimized for pileup and particle type)
(also, see jet algorithms later)

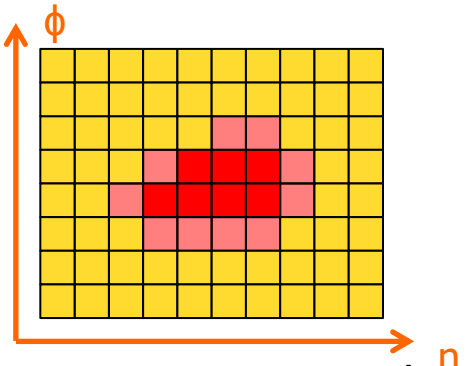

$$E_p = G \cdot F_p\left(\sum_j E_j^{\text{cell}}, \eta, \phi, X, \ldots\right)$$

Energy calibration regression. Depends on many parameters and particle type, today often ML-based. Can contain additional non-uniformity corrections.

Hardware response calibration

- **Electronic calibration** G_j
  - ✓ Equalize and monitor cell-to-cell response and associated electronics, track response time-variations
  - ✓ **Injects known current pulse** at readout chain input
    - Typically at preamplifier level
  - ✓ Channel-to-channel dispersions as small as 0.2% can be achieved → **precision and stability of the calibration system are essential (typically <0.1%)**
  - ✓ For Gain Switching readout (e.g. ATLAS) calibration system plays crucial role in measuring gain offset values
  - ✓ Calibration pulses can be issued regularly during data taking, in allocated time slots without physics
    - e.g. in SPS cycles: calibration time right after the 3-5 physics spill - extra 0.5 s every cycle (14-16 s)
    - e.g. in LHC cycles: using LHC gaps (1 gap of ~ 3μs every ~ 3200 Bunch Crossings)
  - ✓ Longer calibration run during periods with no physics data (e.g. LHC fills)

- **Detector physics calibration** c_j
  - ✓ Electronic calibration does not allow calibration of the detector response
  - ✓ Other devices (e.g. **lasers, radioactive sources**) are used, that inject a well-known light or charge signal into the active elements of the detector
  - ✓ Radioactive sources used to calibrate hadron calorimeters or calorimeter designed for low energies, or to track transparency changes in crystals
  - ✓ **Radioactive sources have well defined decay energy**
    - **e.g. Cobalt-60 (γ: 1.17 + 1.33 MeV)**
    - **e.g. Cesium-137 (γ: 661.7 keV)**

7.7

Test-Beam Calibration

Test-beam calibration

- Test-beam: expose detector modules to beams of known particle type and energy
  - ✓ Provides absolute energy scale traceability to beam spectrometer calibration
  - ✓ Measures cross-talk, signal non-linearity, material budget contributions, …
- The D0 cautionary tale…
  - ✓ D0 at Tevatron (Fermilab): first run without dedicated test-beam calibration
  - ✓ Discovered ~5% shift in absolute EM scale *in-situ* from Z→ee
    - *If you don't calibrate at test beam, you will pay for it with in-situ calibration time…*
- Typical test-beam setups
  - ✓ Electron beam (1-200 GeV): measure absolute EM scale and linearity
  - ✓ Pion beam (same range): measure e/pi ratio and hadronic calibration
  - ✓ Muon beam: check cell-by-cell uniformity (MIP scan)
  - ✓ Note: all single particles… (not jets)
- Transferring test-beam to collider: corrections for material in front, non-uniformity, full detector geometry…

$$F_{\mu A \to \mathrm{MeV}} \quad \frac{1}{f_{\mathrm{samp}}}$$

Example of LHC calorimeter test-beams

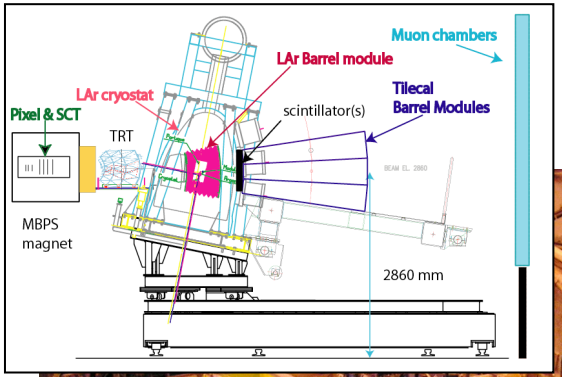

ATLAS combined test-beam 2004

CMS ECAL test-beam 2006

7.8

In-Situ Calibration

Why *in-situ* calibration?

- Every calorimeter needs to be re-calibrated after installation in the experimental hall
  - ✓ Experimental environment (ex. presence of material in front of the calorimeter, geometric deformations) different from test-beam environment, and not probed by hardware calibration
- Calorimeter response to hadron jets and missing transverse energy cannot be measured at test beam where only single particle beans available
  - ✓ Also subtle differences e.g. between electrons and photons, might not be captured at test-beam
- Calibration stability needs to monitored vs time
- **In-situ calibration allows correction of residual non uniformities, to follow detector response variations with time, and to set final absolute energy scale under experimental conditions**
- Tools: well-known control physics samples (with high branching ratios) are used, such as:
  - ✓ Photons: $\pi^0 \rightarrow \gamma\gamma$, $\eta^0 \rightarrow \gamma\gamma$, $Z \rightarrow ee\gamma$ / $\mu\mu\gamma$
  - ✓ Electrons: $J/\psi \rightarrow ee$, $Z \rightarrow ee$, $W \rightarrow e\nu$
  - ✓ Jets: $W \rightarrow jj$, $Z+j$ / $j\gamma$ (Z/photon-jet balance)
  - Muons: : $J/\psi \rightarrow \mu\mu$, $Z \rightarrow \mu\mu$
    - ✓ Muons calibrate response to ionization energy (MIP)
    - ✓ Perfect to calibrate calorimeters with longitudinal segmentation, with EM and HAD parts
  - ✓ For fixed target experiments: calibrated electron beams (in a test-beam like setup)

Standard candles to set absolute energy scale

Particle	Mass	± error	Γ (or τ)	Calibration decay	BR
π^0	134.9768 MeV	0.0005 MeV	$\tau = (8.43 \pm 0.13) \times 10^{-17}$ s	$\pi^0 \to \gamma\gamma$	98.82%
η	547.862 MeV	0.017 MeV	1.31 ± 0.05 keV	$\eta \to \gamma\gamma$ $\eta \to \pi^0\pi^0\pi^0$ / $\pi^+\pi^-\pi^0$	39.36% 32.56% / 23.02%
J/ψ	3096.900 MeV	0.006 MeV	92.6 ± 1.7 keV	$J/\psi \to e^+e^-$ / $\mu^+\mu^-$	5.97% / 5.96%
Z	91.1880 GeV	0.0020 GeV	2.4955 ± 0.0023 GeV	$Z \to e^+e^-$ / $\mu^+\mu^-$ / $\tau^+\tau^-$ $Z \to e^+e^-\gamma$ / $\mu^+\mu^-\gamma$ †	3.37% each QED FSR †
W	80.3692 GeV	0.0133 GeV	2.14 ± 0.05 GeV	$W \to e\nu$ / $\mu\nu$	10.71% / 10.63%

$\Gamma = \hbar/\tau$ · PDG 2025: S. Navas et al., Phys. Rev. D 110, 030001 (2024) + 2025 update

† $Z \to \ell\ell\gamma$ rate is QED FSR, E_γ-dependent (PDG upper limit < 3.2 × 10 $^{-3}$ for specific E_γ range)

Muons as MIPs for calibration

- **Why muons?**
  - ✓ At GeV energies muons are MIP: energy loss follows Bethe-Bloch (~1–2 MeV/cm in typical absorbers)
  - ✓ No EM or hadronic shower: deposit is small, local, layer-by-layer;
  - ✓ Energy deposit per cell: **Landau distribution** → calibration reference = Most Probable Value (MPV)
  - ✓ Sources: isolated muons from $Z \to \mu\mu$ (in-situ, collision data); cosmic muons (commissioning, technical stops)

- **Calibration procedure**
  - ✓ Select isolated muons (pT > 20 GeV); extrapolate track to each calorimeter cell
  - ✓ Fit energy deposit: Landau ⊗ Gaussian convolution (Landau shape + electronic noise smearing)
  - ✓ Extract MPV per cell → compare across cells (uniformity map) or vs. time (stability)
  - ✓ Precision: ~1% per cell with O(100) muons per cell

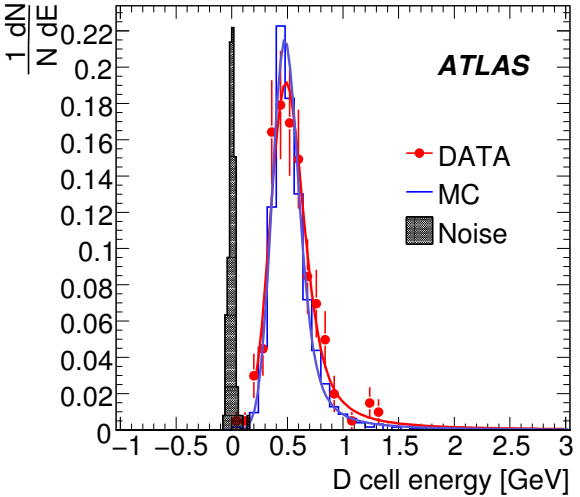

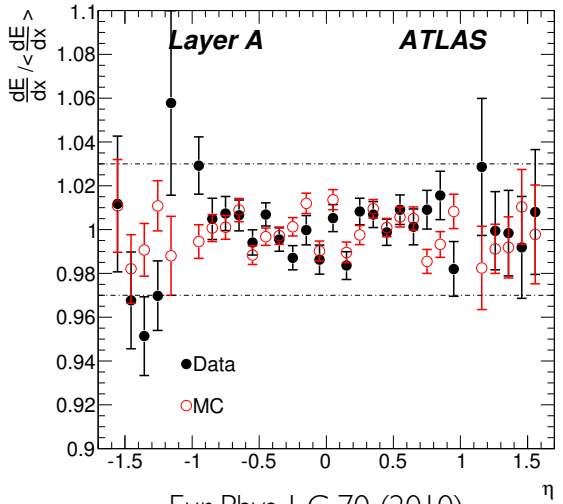

Eur. Phys. J. C 70 (2010)

Muon calibration: longitudinal segmentation and time stability

- **Longitudinal inter-calibration**
  - ✓ Muons deposit energy in **all calorimeter longitudinal layer (EM+HAD)**
  - ✓ MPV ratio between layers → relative EM/HAD inter-scale
  - ✓ E/p consistency: tracker momentum vs. layer-by-layer deposit; useful to identify dead material or uninstrumented regions

Example: ATLAS LAr EM Layer 1 / Layer 2 response as seen by muons

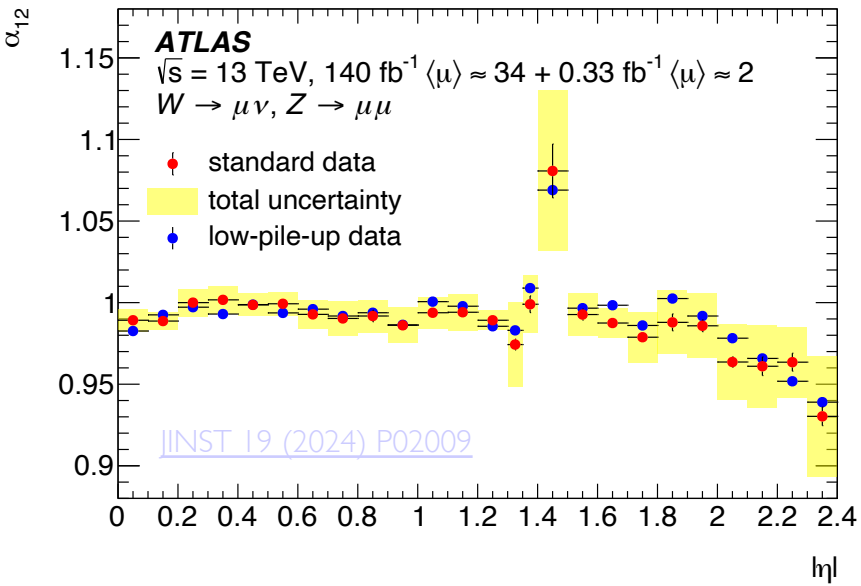

- **Time stability monitoring**
  - ✓ Track MPV vs. run number / integrated luminosity: sensitive to gain drift, radiation damage, HV instability
  - ✓ Independent cross-check of laser and radioactive source monitoring: muons probe the *full* signal chain (detector + electronics), not just optics or injection point
  - ✓ Cosmic muon runs available during technical stops when when accelerator not delivering collisions (even before data taking)

EM in-situ calibration: $\pi^0 \to \gamma\gamma$ and $Z \to ee$

- **$\pi^0 \to \gamma\gamma$ / $\eta^0 \to \gamma\gamma$**
  - ✓ Abundant
  - ✓ Known mass (135 MeV, 547.8 MeV)
  - ✓ calibrate individual cells by fitting diphoton invariant mass peak
  - ✓ Precision: ~ 0.5% per cell after ~ 100 pb^{-1} (used at beginning of data taking)
- **$Z \to ee$**
  - ✓ Gold standard for absolute EM energy scale
  - ✓ Known Z mass (91.2 GeV).
  - ✓ Fit Z mass peak as function of eta
    - Initially apply ϕ-symmetric corrections
    - With larger statistics: ϕ-dependent modulation, E_T-dependent corrections
  - ✓ Achieves < 0.02% inter-channel uniformity after full in-situ campaign

$$E_i^{\mathrm{corr}} = E_i/(1+\alpha_i)$$

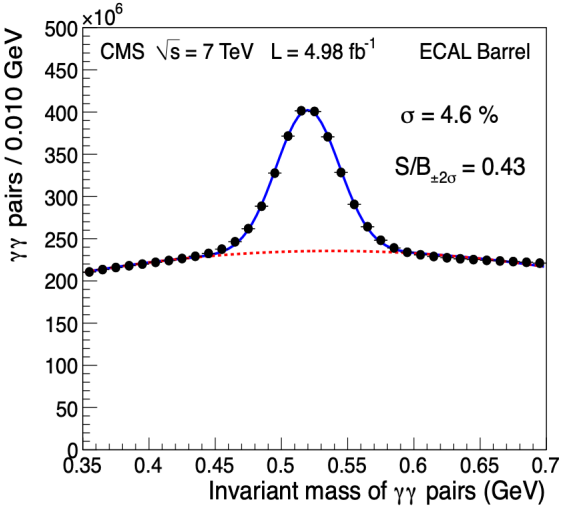

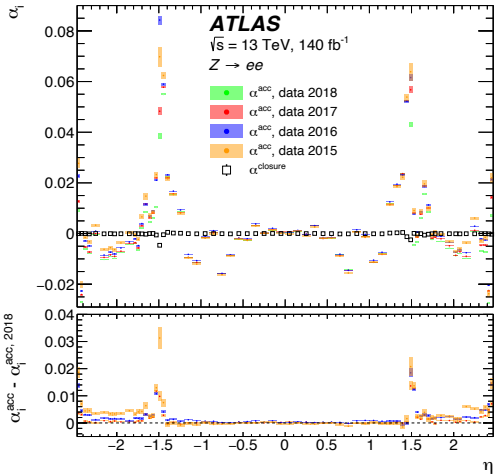

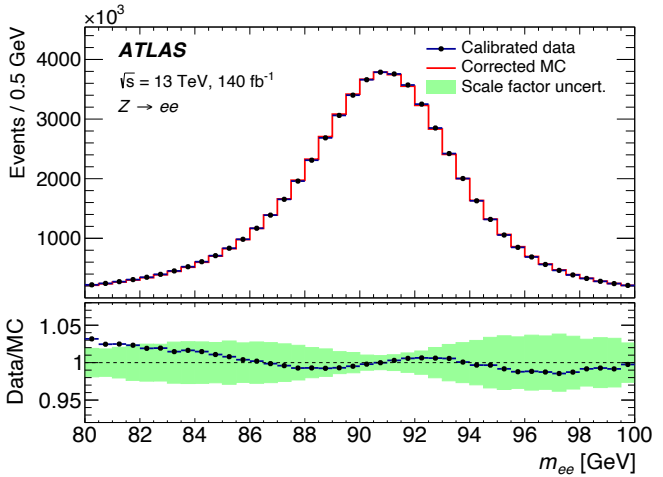

EM in-situ calibration: E/p method

- E/p method: compare calorimeter E to tracker p for isolated electrons.
  - ✓ $E_{ECAL} / p_{tracker} = 1$ for electron → deviations reveal local mis-calibration or material effects
  - ✓ $p_{tracker}$ momentum calibrated e.g. by using isolated muons from $Z \rightarrow \mu\mu$
- Procedure
  - ✓ Simulation of tracker material distribution used to compute electron energy losses (bremsstrahlung) and obtain initial electron momentum
  - ✓ Momentum scale then transferred to calorimeter by adjusting the *E/p* distribution MPV for electrons to 1

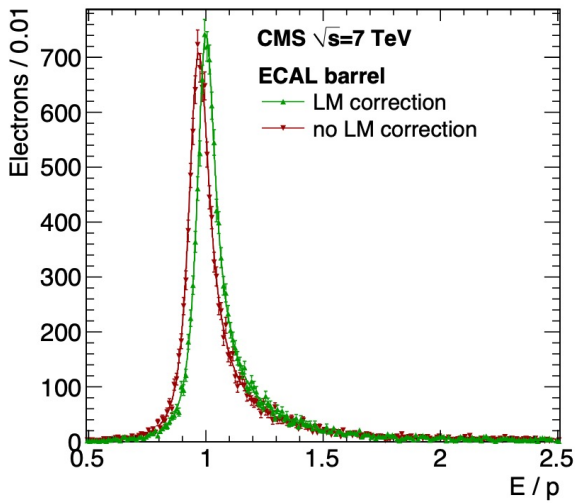

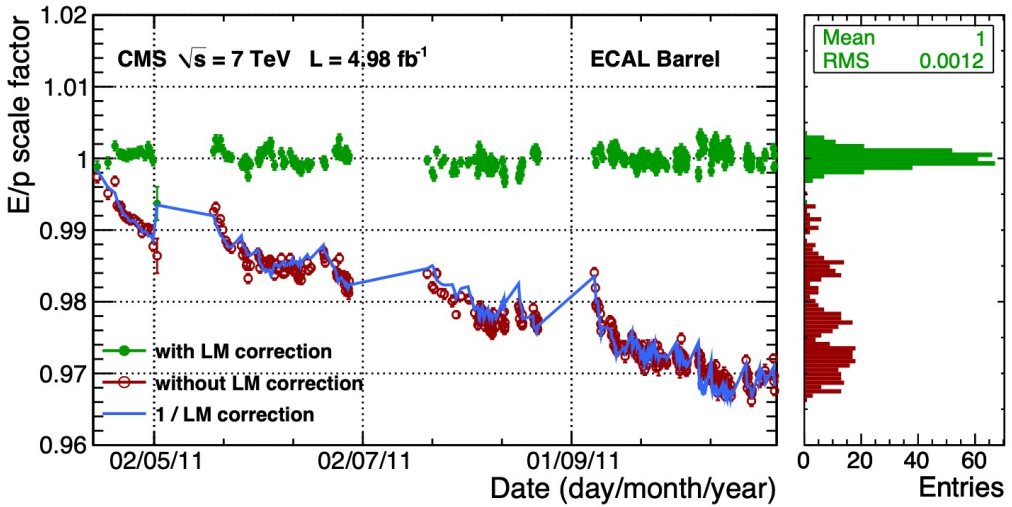

The D0 cautionary tale…

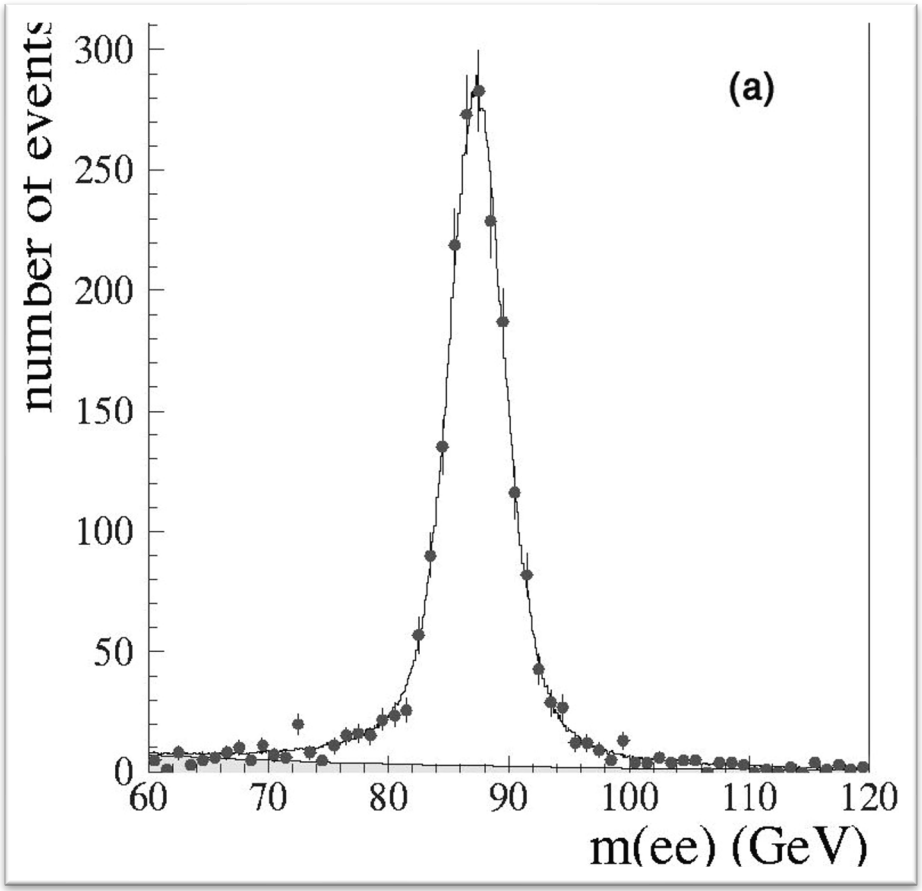

di-electron mass spectrum reconstructed in the D0 central calorimeter before the final energy scale calibration (Abbott et al.,1998)

- Both D0 and CDF ultimately achieved a precision on the absolute electron energy scale of ~0.1%
- Limiting factors (e.g. vs LHC)
  - ✓ Statistics of physics samples used to calibrate Z mass peak or the E/p distribution.
  - ✓ Systematic uncertainties
    - Incomplete knowledge of the dead material
    - calorimeter response nonlinearities
    - Treatment of radiative Z decays ($Z \rightarrow ee\gamma$ with low energy undetected photons)

7.9

HAD Calibration

What we already covered…

- **L4 → e/h problem and software compensation**
  - ✓ e/h ≠ 1 in most sampling calorimeters (Fe ~1.3, Pb ~1.4): energy-dependent response bias
  - ✓ SW comp $W(E/V) = c_1 \cdot \exp(-c_2 \cdot E/V) + c_3$: ~20% hadronic resolution improvement at 50 GeV (ATLAS TileCal)

- **L6 → Particle flow as design philosophy**
  - ✓ Jet energy: ~62% charged hadrons (tracker), ~27% photons (ECAL), ~10% neutral hadrons (HCAL)
  - ✓ High-granularity HCAL built to enable track–cluster separation for PF reconstruction

- **Today: JES in-situ calibration → what remains to be done…**
  - ✓ SW comp fixes per-cell hadronic weights, JES pins the jet-level absolute scale from collision data
  - ✓ Methods: γ+jet pT balance · Z+jet balance · η-intercalibration · JES uncertainty decomposition

Why jets need their own absolute scale: the JES problem

- **Test-beam calibrates single particles, jets are composite**
  - ✓ Variable-composition!
    - ~62% charged hadrons, ~27% photons ($\pi^0 \to \gamma\gamma$), ~10% neutral hadrons
  - ✓ f_{EM} fluctuates event-to-event
  - ✓ quark/gluon-induced jets differ in particle multiplicity → variable response

- **Additional complicating factors**
  - ✓ Pile-up: ~25–200 extra pp interactions deposit energy in the jet cone
    - Subtract with ρ × A method
  - ✓ Dead material, cracks
    - Position-dependent losses ~0.5–1%; forward jets ($|\eta| > 2.5$) harder to calibrate
  - ✓ Punch-through at high p_T: energetic jet deposit energy behind HCAL

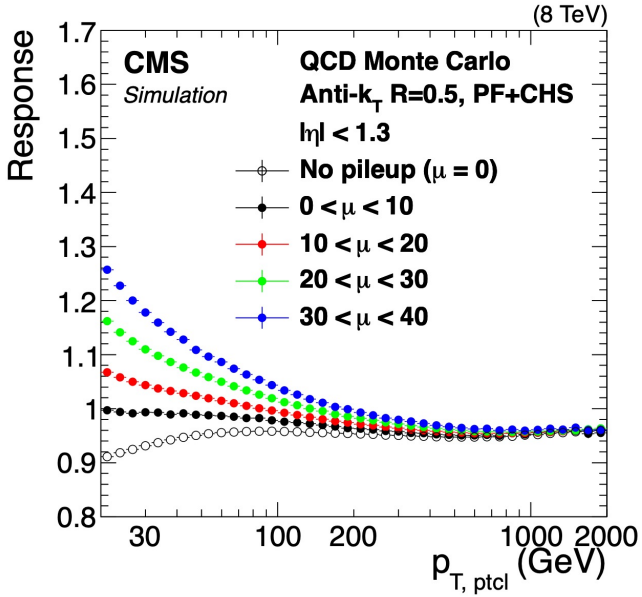

- **Consequence: raw JES offset before in-situ is 10–30% (energy- and η-dependent)**
  - ✓ Target residual uncertainty < 1–2% for central jets…
  - ✓ … a data-driven in-situ correction is unavoidable!

JES in-situ calibration: photon–jet p_T balance

- **Use photon as a precision reference for the jet p_T scale**
  - ✓ Photon p_T known to ~0.1% from EM in-situ

- **Event selection and balance variable**
  - ✓ Select: one isolated γ + one jet, back-to-back in ϕ ($\Delta\phi_{\gamma j} > \pi - 0.2$); veto on additional jets
  - ✓ Balance variable: $\alpha_{pT} = p_T(\text{jet})/p_T(\gamma) \rightarrow$ bin in pT(γ) and η(jet); fit distribution peak
  - ✓ Derive multiplicative correction $c(p_T, \eta)$
    - covers pT ~ 30 GeV to 1 TeV
    - precision ~0.1–0.5% per bin
  - ✓ Procedure: absolute scale first (central barrel $|\eta| < 1.3$), then η-dependent residuals

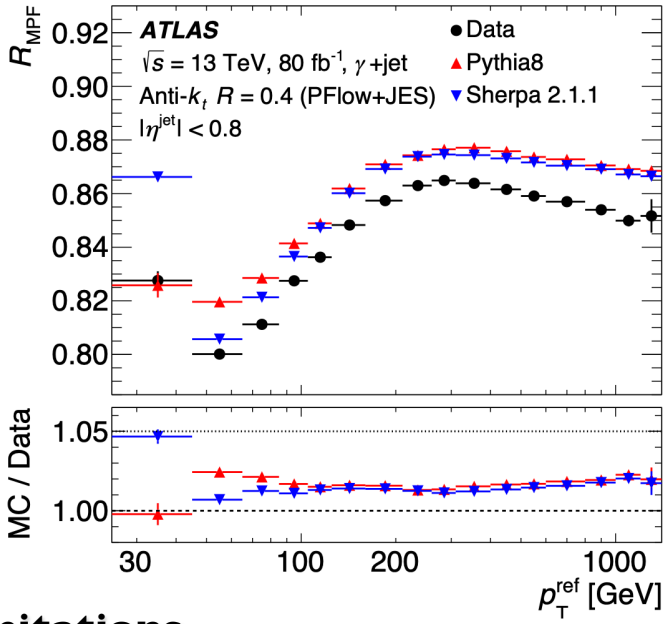

- **Limitations**
  - ✓ γ+jet dominated by quark jets
    - flavor bias for gluon jets
  - ✓ statistics limited at p_T > 1 TeV
    - Z+jet and multijet needed

Z+jet balance, η-intercalibration, and high-p_T extension

- **Z+jet balance: independent calibration with complementary systematics**
  - ✓ Z→ee or Z→μμ: lepton pT known to ~0.1–0.2%; same α_pT = pT(jet)/pT(Z) method
  - ✓ More quark-enriched jet sample than γ+jet → reduces gluon jet flavour bias
  - ✓ Combined γ+jet + Z+jet: cancels correlated systematics, tighter total uncertainty

- **η-intercalibration: extending calibration to forward jets (|η| > 2.5)**
  - ✓ Dijet events: one central jet (|η| < 1.3) as reference, one forward jet as probe
  - ✓ Use pT conservation to derive forward correction; reaches |η| ~ 4.5; precision ~1–2%
  - ✓ Critical for VBF Higgs searches, forward jet veto in WH, and inclusive dijet spectra

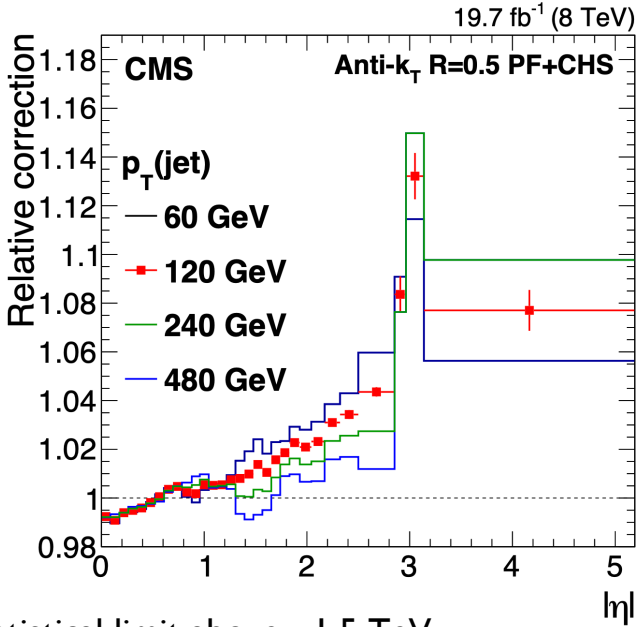

- **Multijet balance: extending to p_T > 1 TeV**
  - ✓ High-pT probe jet recoils against several calibrated low-pT jets; statistical limit above ~1.5 TeV

JES uncertainty: anatomy and physics impact

- **JES uncertainty: independent components added in quadrature**
  - ✓ In-situ statistics: dominant at pT > 1 TeV; drives need for full Run 2/3 dataset
  - ✓ Pile-up residual: ρ × A leaves ~0.5–1% bias at low pT or high <μ>
  - ✓ Flavor composition + response: quark vs. gluon differ by ~5%; gluon fraction from MC
  - ✓ b-jet: neutrino loss from semi-leptonic b-decay → separate b-JES from $t\bar{t}$→bjj events
  - ✓ Dead material, cracks, punch-through: each ~0.5–1% depending on pT and η region

- **Typical total JES uncertainty (ATLAS/CMS Run 2)**
  - ✓ Central jets |η| < 2.5, pT = 30–500 GeV: ~1–2% total
  - ✓ Forward 2.5 < |η| < 4.5: ~3–5%; grows again above ~1 TeV (statistics)
  - ✓ Physics impact: leading systematic in MET resolution · top mass (δm_top ~ 0.5 GeV/1% JES) · VBF Higgs · dijet spectra

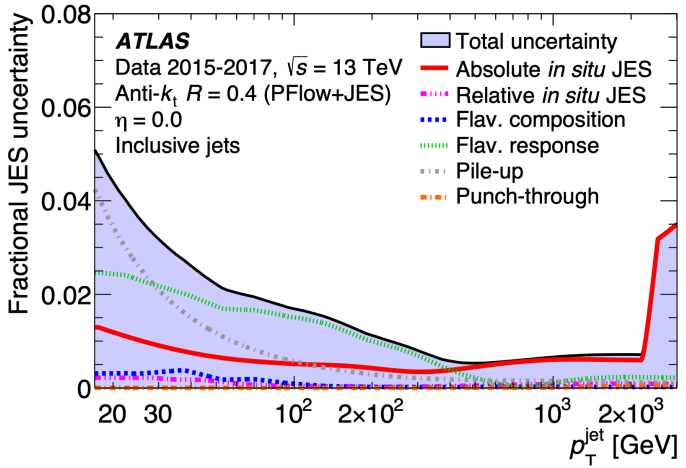

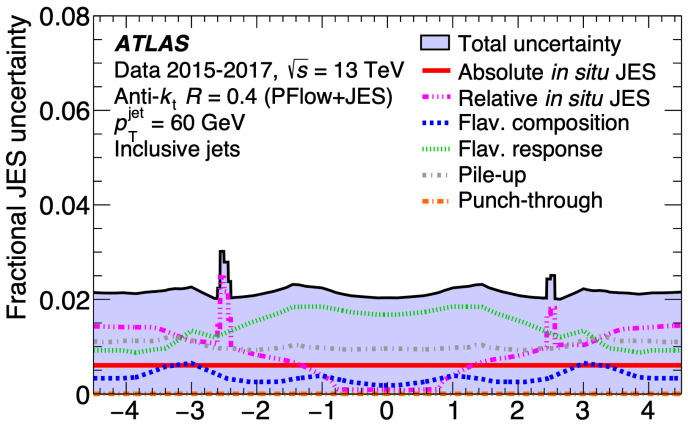

Particle flow: how it reshapes the JES picture

Neutral hadron component limits JES precision at high p_T

At pT > 500 GeV: tracker contribution saturates: HCAL neutral hadron tail dominates residual JES

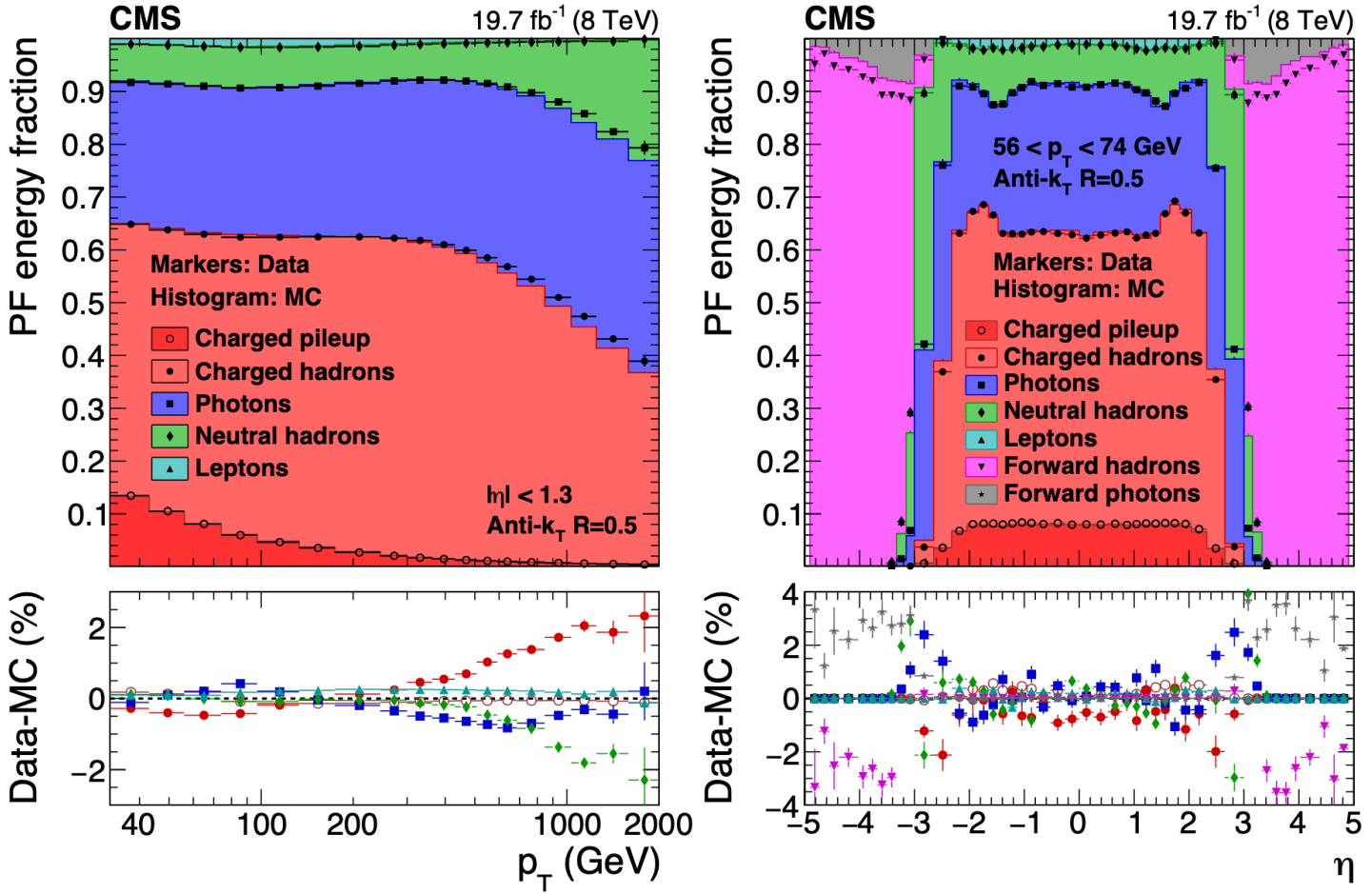

What did we learn today?

- Week 4 (Systems & Future)
  - ✓ Lecture 7: Signal chain, readout, calibration
    - *Signal chain and electronics → from shower energy deposit to ADC counts.*
      - *Signal formation: a shower produces ionization charge (LAr) or scintillation light; triangular LAr current shaped into bipolar voltage pulse for sampling and zero baseline*
      - *Preamplifier & shaping: CSA converts detector charge to voltage ($V = Q/Cf$); CR-RC^n shaping reduces noise bandwidth; peaking time trades noise vs. pile-up; ENC sets minimum detectable energy*
      - *Dynamic range: covering MeV (noise) to TeV (high-pT jets) requires multi-gain readout (intercalibration); ADC quantizes each gain separately*
      - *Optimal filtering: OFC coefficients minimize noise (including pileup) while extracting amplitude and time from a few samples; extreme pile-up at HL-LHC forces ML-based alternatives.*
      - *Trigger primitives: L1 decisions are made in microseconds on coarse trigger-tower sums, but newer electronics allows for better granularity at L1 not individual cells.*
    - *EM and HAD calibration → from ADC counts to calibrated energy to objects*
      - *Calibration chain: energy formula encodes calibration layers: electronics, detector physics response, sampling, global scale)*
      - *Test-beam provides indispensable absolute energy scale traceable to beam spectrometer*
      - *Muon MIP: isolated muons ($Z \to \mu\mu$, cosmics) calibrate cells via Landau MPV; probe full signal chain and monitor stability vs. time*
      - *EM in-situ can pin the absolute EM scale to < 0.02% uniformity*
      - *HAD calibration: cell weighting and software compensation partially recover the non-compensation penalty, but in-situ JES corrections via gamma+jet and Z+jet balance necessary; particle flow unifies design and calibration*
  - ✓ Lecture 8: Future calorimetry